Supplemental Information Inventory

List of Tables

List of Figures

Table S1: Related to Figures 2, 3, 4, 6, and 7. **Simulation parameter values used in main figures.**

	β_I	β_P	β_D	μ	η	θ	γ_1	β_C	γ_C	K_C	β_{P*}
Fig.	min^{-1}	min^{-1}	min^{-1}	min^{-1}	nM^{-1} min^{-1}	min^{-1}	min^{-1}	min^{-1}	nM	nM	nM min^{-1}
2A	0.06	0	0	1	0.01	0.3	0.1	0.1‡	0.1	–	–
2B	0.06	0	0	1	0.01	0.3	0.1	0.1‡	0.1	300	90
2C	0.06	0	0	1	0.01	0.3	0.1	0.1‡	0.1	–	90
2D	0.06	0.3	0	1	0.01	0.3	0.1	0.1‡	0.1	–	–
3A	0.06	0	0.56	1	0.01	0.3	0.1	0.1‡	0.1	–	–
3B	0.06	0	0.56	1	0.01	0.3	0.1	0.1‡	0.1	–	–
3C	0.06	0	0.56	1	0.01	0.3	0.1	0.1‡	0.1	–	–
3D	0.06	0.15	0.28	1	0.01	0.3	0.1	0.1‡	0.1	–	–
4	0.06	0.15	0.28	1	0.01	0.3	0.1	0.1	0.1	–	–
6	†	†	†	1	0.01	0.3	0.1	0.1‡	0.1	–	–
7A	0.0576*	0	0	1	–	0.3	0.1	0.1‡	0.1	–	–
7B	0.0576*	0.15	0.28	1	–	0.3	0.1	0.1‡	0.1	–	–

	γ_{A_0}	β_A	γ_A	γ_M	K_A	K_M	β_{M*}	β_M	β_Z	γ_Z	K_Z
Fig.	min^{-1}	min^{-1}	min^{-1}	min^{-1}	nM	nM	nM min^{-1}	min^{-1}	min^{-1}	min^{-1}	nM
2A	–	–	–	–	–	–	–	–	–	–	–
2B	–	–	–	–	–	–	–	–	–	–	–
2C	–	–	–	–	–	–	–	–	–	–	–
2D	–	–	–	–	–	–	–	–	–	–	–
3A	0.1	1.5	1.5	1.5	1	1	–	0.4167	–	–	–
3B	0.1	1.5	1.5	1.5	1	1	125	–	–	–	–
3C	0.1	1.5	1.5	1.5	1	1	–	0.4167	–	–	–
3D	0.1	1.5	1.5	1.5	1	1	–	0.4167	–	–	–
4	0.1	1.5	1.5	1.5	1	1	–	0.4167	–	–	–
6	0.1	1.5	1.5	1.5	1	1	–	0.4167	–	–	–
7A	–	–	–	–	–	–	–	–	4	2	1
7B	0.1	1.5	1.5	1.5	1	1	–	0.4167	4	2	1

‡ Unless directly perturbed (e.g. $\beta_C = [0.1, 0.15, 0.2]\,\text{min}^{-1}$).
† Multiple values (shown in the figure) were tested.
* Corresponds to β_{I*} parameter in the alternative PID system (see Section "Constructing a PID controller with a different integral controller architecture").

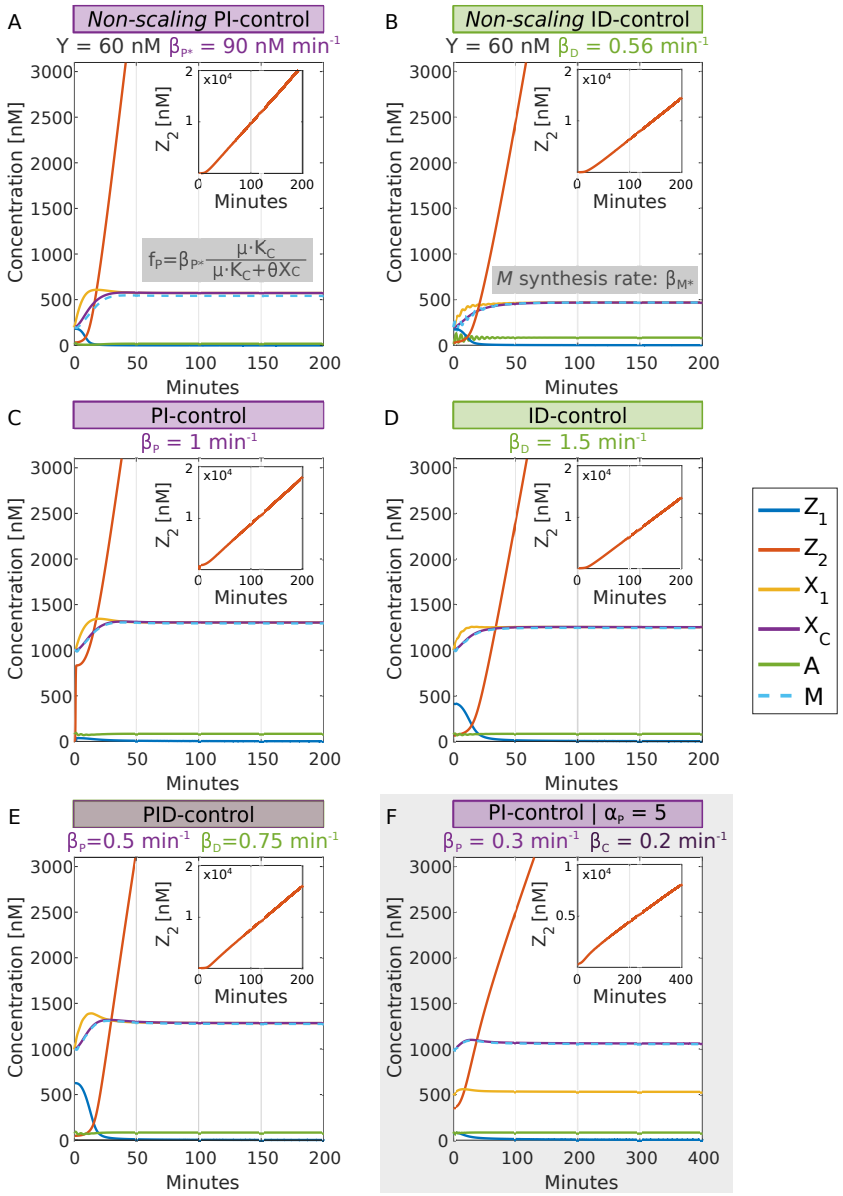

Figure S1: Related to Section "Design of a proportional control term", Section "Design of a derivative control term", and STAR Methods "Bounds on antithetic integral control with P and D terms". **Suboptimal performance occurs when the proportional or derivative controllers are too strong.** Z_2 levels increase linearly over time when the (A,C) proportional, (B,D) derivative, or (E) a combination of these are too strong and the production of Z_1 is too small to compensate for the production of Z_2. This occurs, for example, for low Y set-point values. In all plots the state variables reach a steady-state except for Z_2. (A,B) Plots of all state variables for controllers in which the proportional (A) or derivative (B) terms do not scale with the set-point Y. In these cases, $Y = 60$ nM is too small for the strength of the proportional and derivative functions, respectively (see Figure 2A and Figure 3B). (C-E) Plots of all state variables for controllers PI and ID designed in this work, in which controller scales with set-point Y. When β_P and β_D, or a combination of these, are too high, loss of integral function is also observed. (F) When $\alpha_P \neq \mu/\theta$ is too high (see Figure S2C), loss of integral control also occurs. See Table S2 for parameter values used in each simulation.

Table S2: Related to Sections "Design of a proportional control term", "Design of a derivative control term", and "Linear perturbation analysis of nonlinear PID control design provides analytical support for the design", and Figures 2, 3, and 4. **Simulation parameter values used in supplementary figures.**

	β_I	β_P	β_D	μ	η	θ	γ_1	β_C	γ_C	ϵ_C	α_P
Fig.	min^{-1}	min^{-1}	min^{-1}	min^{-1}	nM^{-1} min^{-1}	min^{-1}	min^{-1}	min^{-1}	nM	nM min^{-1}	
S1A	0.06	0	0	1	0.01	0.3	0.1	0.1	0.1	–	–
S1B	0.06	0	0.56	1	0.01	0.3	0.1	0.1	0.1	–	–
S1C	0.06	1	0	1	0.01	0.3	0.1	0.1	0.1	–	–
S1D	0.06	0	1.5	1	0.01	0.3	0.1	0.1	0.1	–	–
S1E	0.06	0.5	0.75	1	0.01	0.3	0.1	0.1	0.1	–	–
S1F	0.06	0.3	0	1	0.01	0.3	0.1	0.2	0.1	–	5
S2B	0.06	0.3*	0	1	0.01	0.3	0.1	0.1‡	0.1	500	–
S2C	0.06	0.3*	0	1	0.01	0.3	0.1	0.1‡	0.1	–	[...]**
S3A	0.06	0.3	0	1	0.01	0.3	0.1	0.1‡	0.1	–	–
S3B	0.06	0.55	0	1	0.01	0.3	0.1	0.1‡	0.1	–	–
S3C	0.06	0.7	0	1	0.01	0.3	0.1	0.1‡	0.1	–	–
S5	†	†	†	1	0.01	0.3	0.1	0.1‡	0.1	–	–
S6A	0.06	0	0	1	0.01	0.3	0.1	0.1‡	0.1	–	–
S6B	0.06	0.3	0	1	0.01	0.3	0.1	0.1‡	0.1	–	–
S6C	0.06	0	0.56	1	0.01	0.3	0.1	0.1‡	0.1	–	–
S7A	0.06	0.3	0.28	1	0.01	0.3	0.1	0.1‡	0.1	–	–
S7B	0.06	0	0	1	0.01	0.3	0.1	0.1‡	0.1	–	–
S7C	0.06	0.3	0.28	1	0.01	0.3	0.1	0.1‡	0.1	–	–

	γ_{A_0}	β_A	γ_A	γ_M	K_A	K_M	β_{M*}	β_M	K_C	β_{P*}	K_{X_1}
Fig.	min^{-1}	min^{-1}	min^{-1}	min^{-1}	nM	nM	nM min^{-1}	min^{-1}	nM	nM min^{-1}	nM
S1A	–	–	–	–	–	–	–	–	300	90	–
S1B	0.1	1.5	1.5	1.5	1	1	125	–	–	–	–
S1C	–	–	–	–	–	–	–	–	–	–	–
S1D	0.1	1.5	1.5	1.5	1	1	–	0.4167	–	–	–
S1E	0.1	1.5	1.5	1.5	1	1	–	0.4167	–	–	–
S1F	–	–	–	–	–	–	–	–	–	–	–
S2B	–	–	–	–	–	–	–	–	–	–	–
S2C	–	–	–	–	–	–	–	–	–	–	–
S3A	–	–	–	–	–	–	–	–	–	–	1
S3B	–	–	–	–	–	–	–	–	–	–	1
S3C	–	–	–	–	–	–	–	–	–	–	1
S5	0.1	1.5	1.5	1.5	1	1	–	0.4167	–	–	–
S6A	–	–	–	–	–	–	–	–	–	–	–
S6B	–	–	–	–	–	–	–	–	–	–	–
S6C	0.1	1.5	1.5	1.5	1	1	–	0.4167	–	–	–
S7A	0.1	1.5	1.5	1.5	1	1	–	0.4167	–	–	–
S7B	–	–	–	–	–	–	–	–	–	–	–
S7C	0.1	1.5	1.5	1.5	1	1	–	0.4167	–	–	–

‡ Unless directly perturbed (e.g. $\beta_C = [0.1, 0.15, 0.2]\,\text{min}^{-1}$).

* Except when stated otherwise.

** Multiple values: $\alpha_P = [0.5, 0.75, 1, 1.25, 1.5]\,\frac{\mu}{\theta}$.

† Multiple values (shown in the figure) were tested.

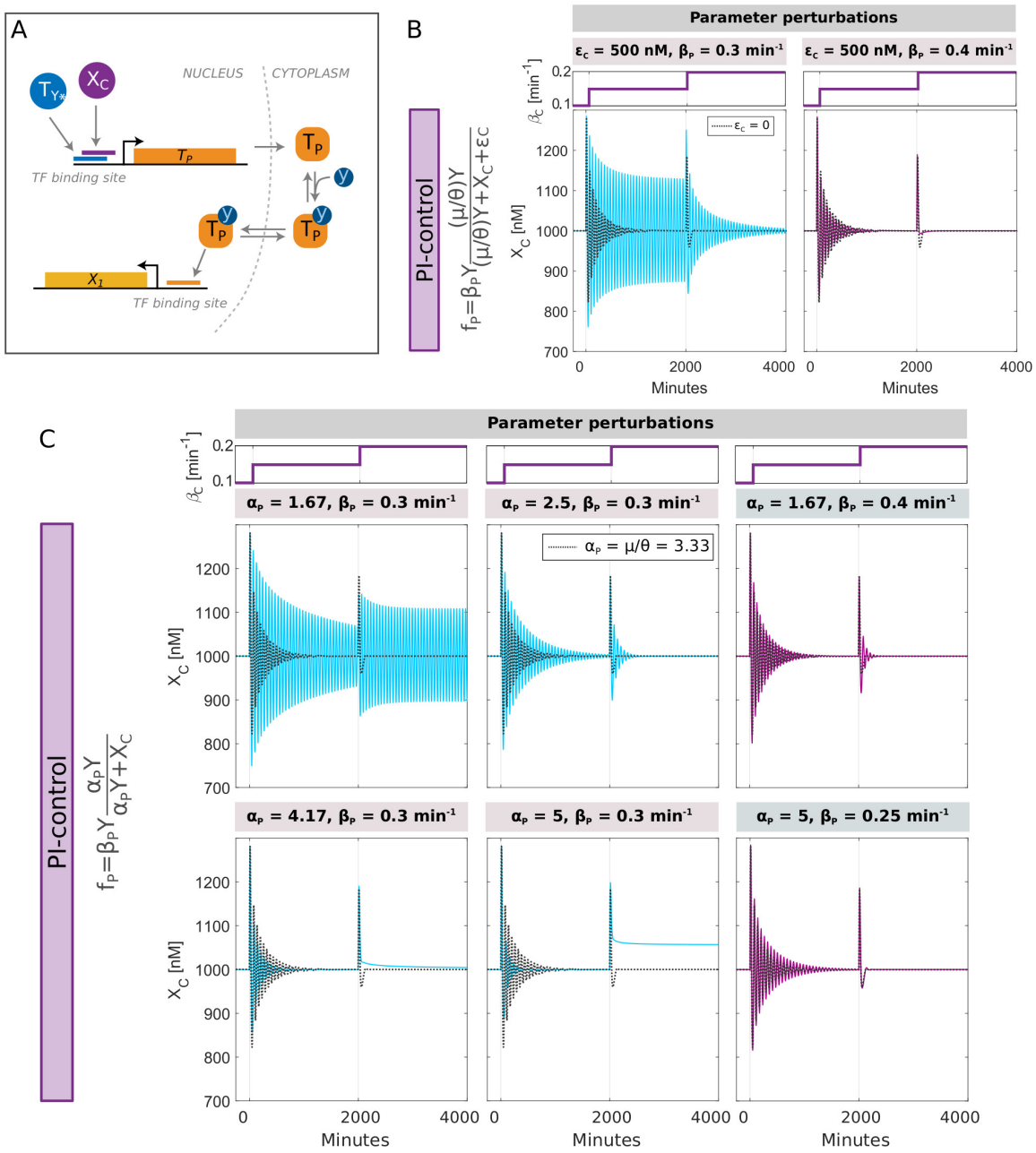

Figure S2: Related to Section "Design of a proportional control term" and STAR Methods "Experimental realization of proportional control function". **Proportional function realization and non-ideal cases.** (A) Proposed experimental realization of the proportional control function $f_P(X_C, Y) = \beta_P Y \frac{\alpha_P Y}{\alpha_P Y + X_C + \epsilon_C}$ (Eq. s4). (B) [Left panel] Time dynamics of output $X_C(t)$ following a change in process parameter β_C for $Y = 300\,\text{nM}$ in a model with a PI controller when $\alpha_P = \mu/\theta = 3.33$ and $\epsilon_C = 500\,\text{nM}$. The example with $\epsilon_C = 0$ is shown on the same plot as a dotted line for comparison. [Right panel] Same plot with $\epsilon_C = 500\,\text{nM}$, but for an increased value of β_P from $\beta_P = 0.3\,\text{min}^{-1}$ to $\beta_P = 0.4\,\text{min}^{-1}$. In general, increasing ϵ_C weakens the proportional feedback, but this effect can be compensated for by increasing the value of the proportional weight β_P. (C) Time dynamics of output $X_C(t)$ following a change in process parameter β_C for $Y = 300\,\text{nM}$ in a model with a PI controller when $\alpha_P \neq \mu/\theta$ and $\epsilon_C = 0\,\text{nM}$. In all cases, the example with $\alpha_P = \mu/\theta = 3.33$ is shown as a dotted line for comparison. Last column showing different values of β_P illustrates that decreasing α_P weakens the proportional feedback and that this effect can be compensated for by increasing the value of β_P. However, for large enough α_P (e.g. $\alpha_P = 5$), the integral controller is compromised (see Figure S1F for Z_1 and Z_2 dynamics). But, this again can be compensated for by decreasing β_P. This illustrates the iterative design process that should be undertaken in these systems. See Table S2 for parameter values used in each simulation.

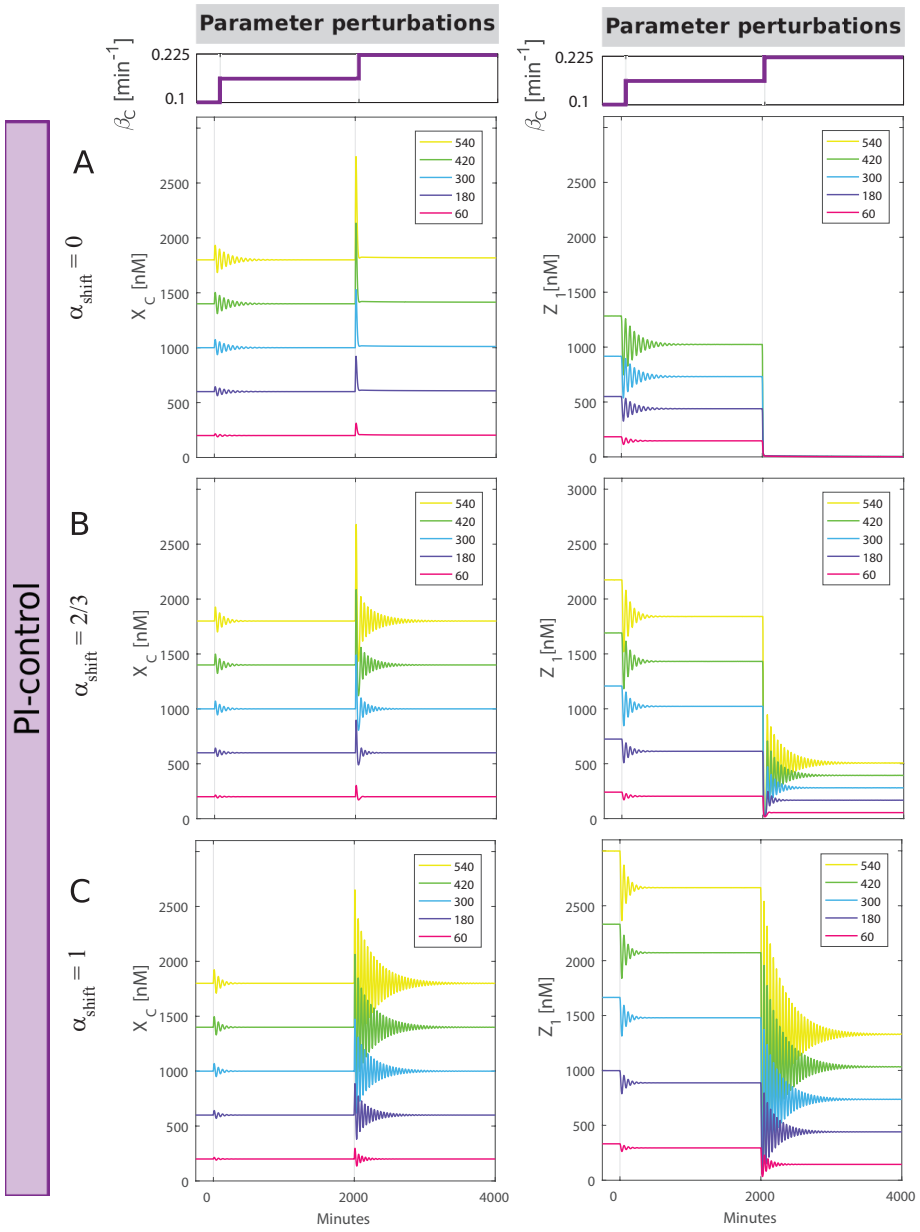

Figure S3: Related to Section "Design of a proportional control term" and STAR Methods "Adding active degradation to the X_1 equation". **Adding active degradation in proportional control can help extend dynamic range of operation.** Time dynamics of X_C and Z_1 following positive step changes in β_C (starting at $0.1\,\mathrm{min}^{-1}$ with subsequent step changes to $0.1125\,\mathrm{min}^{-1}$, and then $0.225\,\mathrm{min}^{-1}$) for (A) $\alpha_{\mathrm{shift}} = 0$, (B) $\alpha_{\mathrm{shift}} = 2/3$, and (C) $\alpha_{\mathrm{shift}} = 1$ in Eq. (s5). Each color represents a different value of Y used ([nM]; see legend). See Table S2 for parameter values used in each simulation.

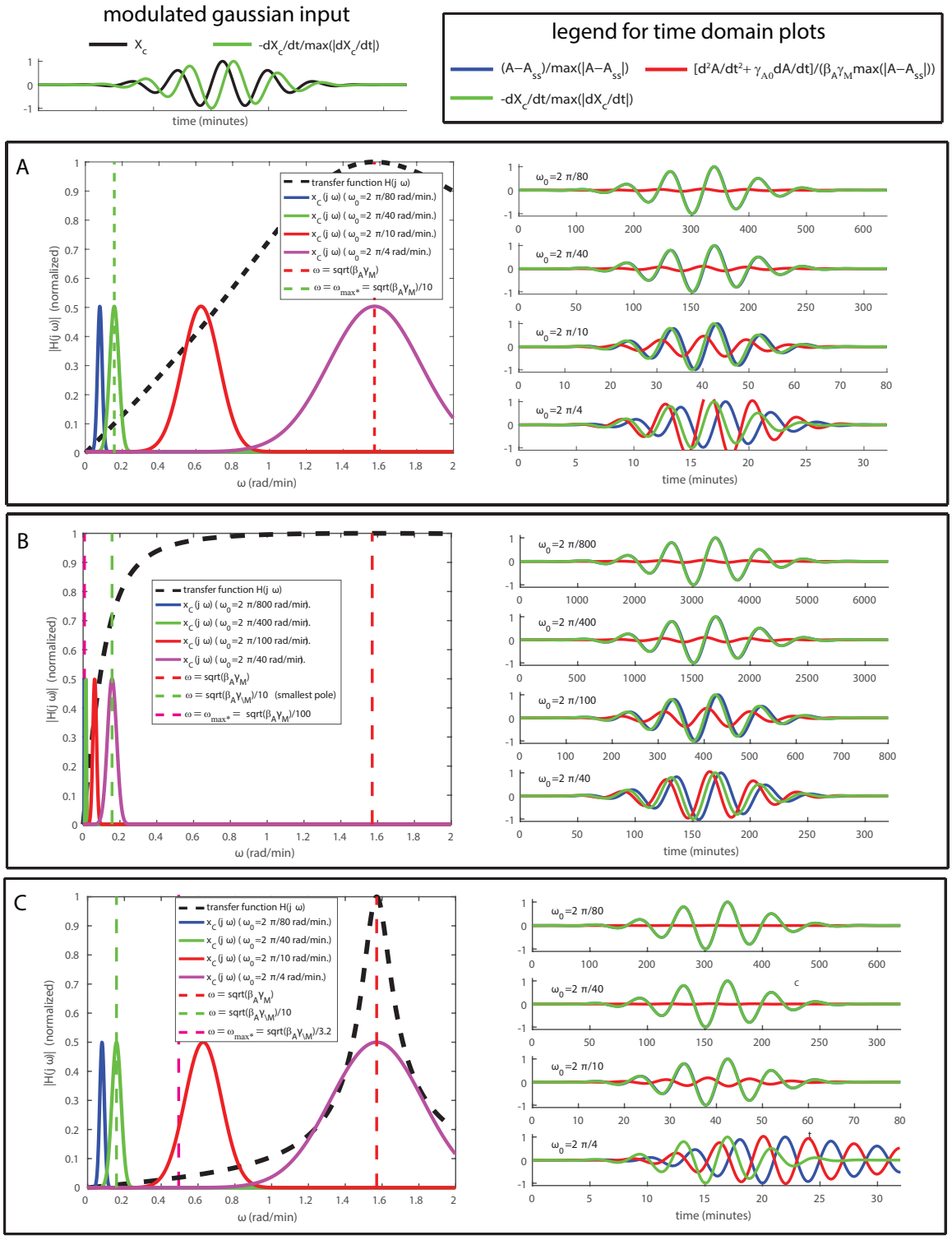

Figure S4: Related to Section "Design of a derivative control term", STAR Methods "Realizing the derivative control term" and STAR Methods "Analysis of poles in Eq.(s7)". **Design choices for the parameter values of derivative motif requires $|-\omega_{max}^2+\gamma_{A_0}\omega_{max}| \leq \beta_A\gamma_M/N$ to ensure accurate derivative measurement.** Top plot (left) displays time-domain X_C (input to the derivative motif) and $-dX_C/dt$. Here $X_C = \exp\left(-\frac{1}{2}(\frac{t-t_0}{\tau})^2\right)\cos\left(\omega_0[t-t_0]\right)$, i.e. a modulated gaussian of width τ and frequency $\omega_0 = 2\pi/\tau$, $t_0 = 4\tau$, and amplitude 1. (Continued on next page.)

Figure S4: (Previous page.) Panels A-C: Left plot displays frequency domain representation of $X_C(j\omega)$ and transfer function $H(j\omega)$ of the derivative motif, where $s = j\omega$. Also plotted are $\omega = \sqrt{\beta_A \gamma_M}$ (fast), $\omega = \sqrt{\beta_A \gamma_M}/10$ (slow) to show where slow, medium and fast time scales (low, medium, and high frequencies) reside, compared with $\omega = \omega_{max^*}$ (also plotted). Right plots: Simulation of Eqs. (13-14). Plotted for comparison are $-dX_C(t)/dt/\max|-dX_C(t)/dt|$ and $(A(t) - A_{ss})/\max|A(t) - A_{ss}|$, i.e. a normalized comparison between $-dX_C(t)/dt$ and $A(t)$. Here A_{ss} represents steady-state A. We also plot $[\frac{d^2A(t)}{dt^2} + \gamma_{A_0}\frac{dA(t)}{dt}]/(\beta_A\gamma_M \max|A(t) - A_{ss}|)$ to visually see if, on average, $|\frac{d^2A}{dt^2} + \gamma_{A_0}\frac{dA}{dt}|$ is much smaller than $|\beta_A\gamma_M A|$. Simulations used parameter values $\gamma_A = 31.4\,\mathrm{min}^{-1}$, $\beta_A = \gamma_M = 1.57\,\mathrm{min}^{-1}$, and $\beta_M Y = 1.57\,\mathrm{nM\,min}^{-1}$. And $\gamma_{A_0} = \sqrt{\beta_A\gamma_M}/K$. From the design constraint in Eq.(s11), we set $N = 10$. where $1/N$ is the relative error tolerance. We also calculated the phase and amplitude of $\frac{\beta_A\gamma_M}{\gamma_A}\frac{\gamma_A}{-\omega^2+\gamma_{A_0}j\omega+\beta_A\gamma_M}$ at the modulation frequency ω_0. This gives us an approximate phase error $\Delta\phi$ and relative amplitude ratio R_{amp} between $A(t)$ and $-dX_C(t)/dt$. (A) Case 1: $K = 1$, $N = 10$. The values for τ, the modulated gaussian parameter, were $\tau = 80, 40, 10$ and 4 minutes. This corresponds to $R_{amp} = 1.001, 1.005, 1.075$, and 1.001. And $\Delta\phi = -2.85\pi/180, -5.80\pi/180, -25.4\pi/180$, and $-90\pi/180$ radians. (B) Case 2: $K = 0.1$, $N = 10$. The values for τ, the modulated gaussian parameter, were $\tau = 800, 400, 100$ and 40 minutes. This corresponds to $R_{amp} = 0.999, 0.995, 0.931$, and 0.709. And $\Delta\phi = -2.92\pi/180, -5.82\pi/180, -21.57\pi/180$, and $-45.46\pi/180$ radians. C) Case 3: $K = 10$, $N = 10$. The values for τ, the modulated gaussian parameter, were $\tau = 80, 40, 10$ and 4 minutes. $R_{amp} = 1.003, 1.010, 1.189$, and 10.004. And $\Delta\phi = -0.29\pi/180, -0.58\pi/180, -2.72\pi/180$, and $-90.0\pi/180$ radians.

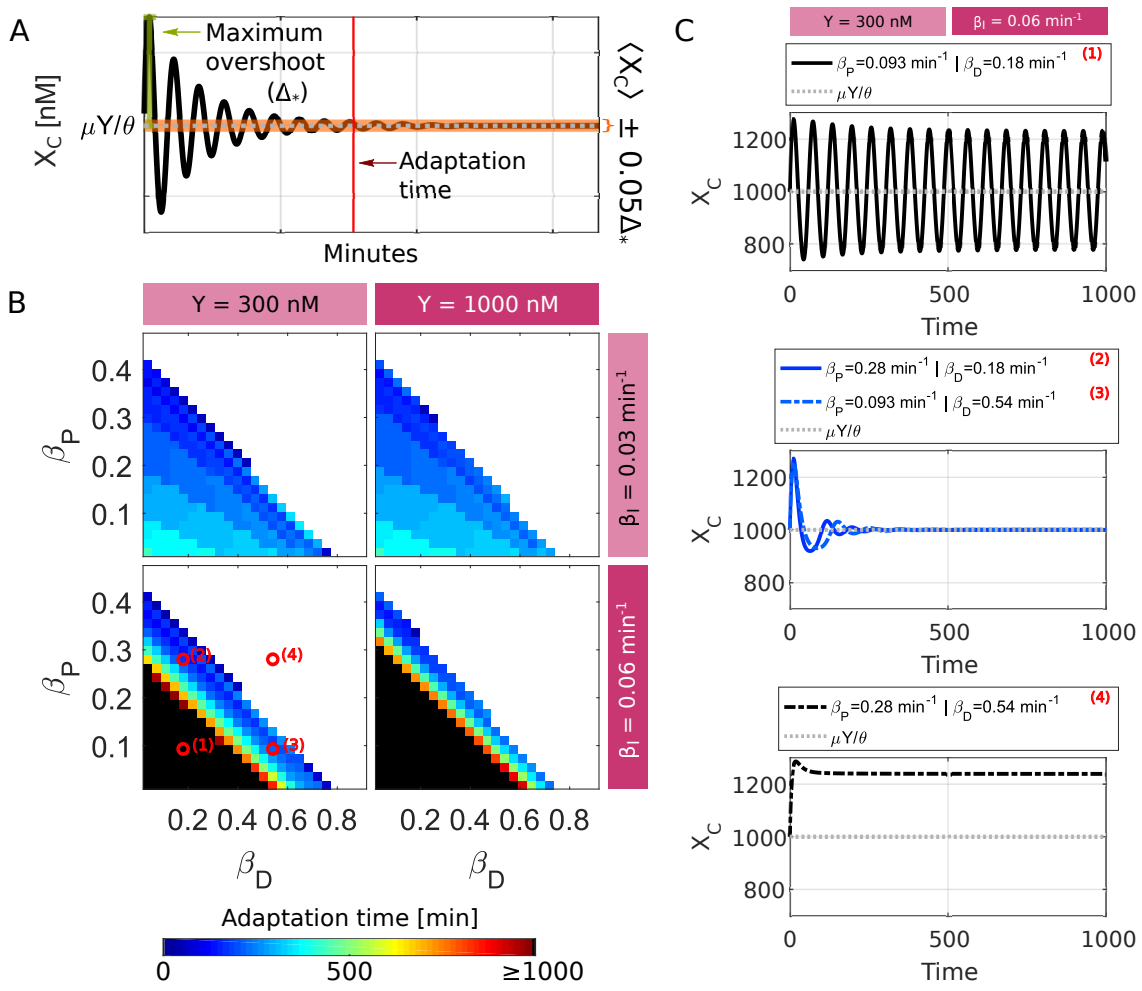

Figure S5: Related to Section "Design of a derivative control term" and STAR Methods "Bounds on antithetic integral control with P and D terms" **Adaptation time as a function of control weights for the simple process (Eq.(5) in main text).** (A) Diagram exemplifying how the adaptation time is calculated. For a given combination of proportional, derivative and integral control weights, a simulation is started from the steady-states for $\beta_C = 0.1\,\text{min}^{-1}$. The value of β_C is then changed to $\beta_C = 0.15\,\text{min}^{-1}$, and the system simulated for 1000 minutes. Following this perturbation to β_C, the system is assumed to have reached steady-state once $X_C = \langle X_C \rangle \pm \varepsilon$, where $\langle X_C \rangle$ corresponds to steady-state of X_C after the perturbation and ε is equal to 5% of the maximum observed "overshoot" or change with respect to $\langle X_C \rangle$. (B) Plot of adaptation time as a function of control parameter weights. Each point on the heat map corresponds to a different value of β_P and β_D, and the color corresponds to the measured adaptation time according to the color-bar on the bottom. The value is shown in white if the system loses adaptation (integral controller is broken, see Figure S1), and in black if adaptation took too long (i.e. more than 1000 minutes). Each panel shows adaptation for a different $Y = [300, 1000]$ nM and $\beta_I = [0.03, 0.06]\,\text{min}^{-1}$. (C) Examples of $X_C(t)$ dynamics for different values of β_P and β_D, with $Y = 300$ nM and $\beta_I = 0.06\,\text{min}^{-1}$ (lower left panel in (B), values of β_D and β_P used for simulations are also marked on this panel). Examples show include a case where stable oscillations are observed (top panel), adaptation is efficiently achieved (middle panel), and the system loses integral control (bottom panel; Z_1 is too small to control Z_2; Figure S1). See Table S2 for parameter values used in these simulations.

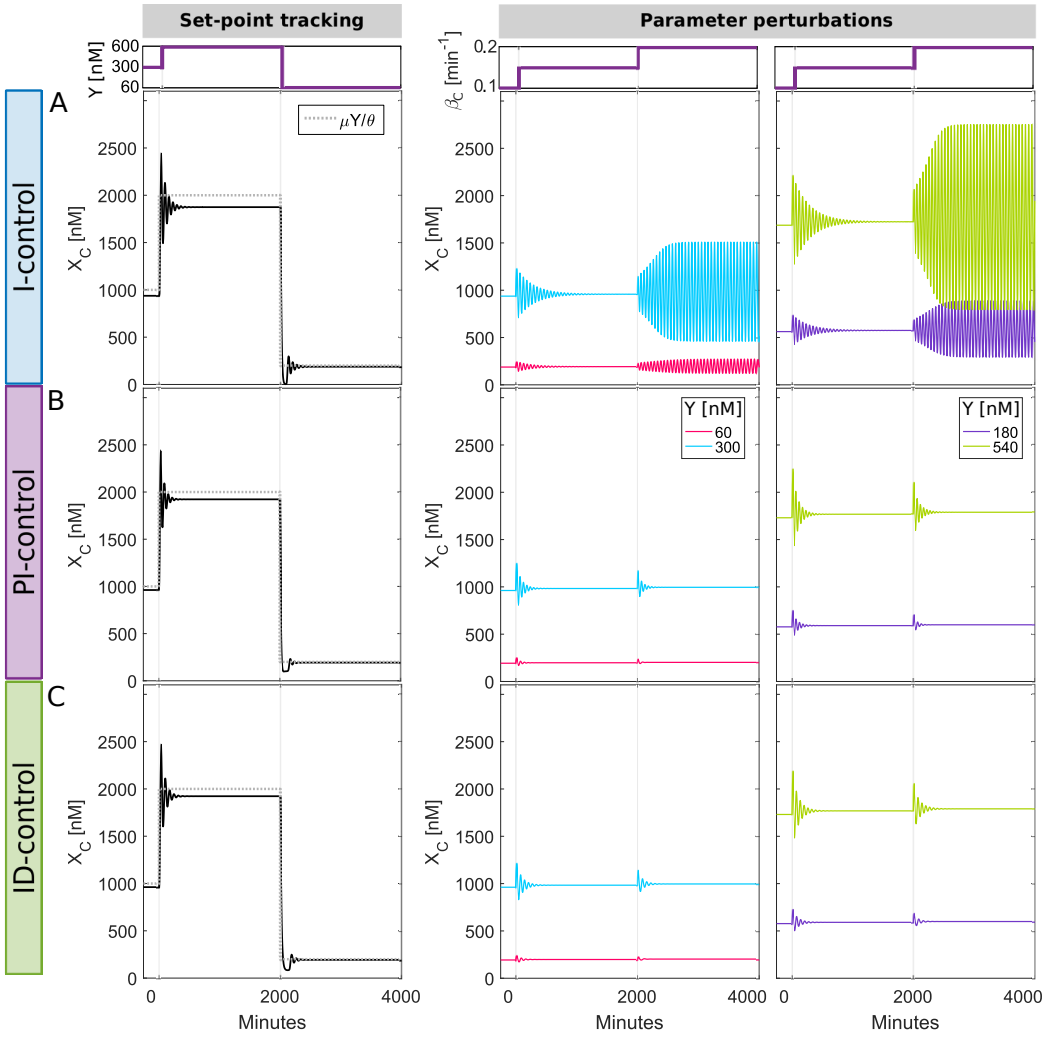

Figure S6: Related to Section "Design of a derivative control term". Related to Figures 2 and 3. **Proportional and derivative control terms improve steady-state adaptation error in the presence of dilution.** (A) Time dynamics of output $X_C(t)$ following a change in the set-point Y (left panel) or in process parameter β_C (right panel). The outcome of β_C perturbation is also shown for different values of $Y = [60, 180, 300, 540]$ nM. Simulations are shown for process in Eq.(5) and antithetic integral controller design in Eqs.(6-8) (I control; $f_P(X_C, Y) = 0$ and $D_t(X_C, Y) = 0$). (B) Time dynamics of output $X_C(t)$ with proportional control (PI control; $D_t(X_C, Y) = 0$). (C) Time dynamics of output $X_C(t)$ with derivative control (ID control; $f_P(X_C, Y) = 0$). For all cases the dilution rate is $\gamma_d = 0.01\,\text{min}^{-1}$. See Table S2 for parameter values used in each simulation.

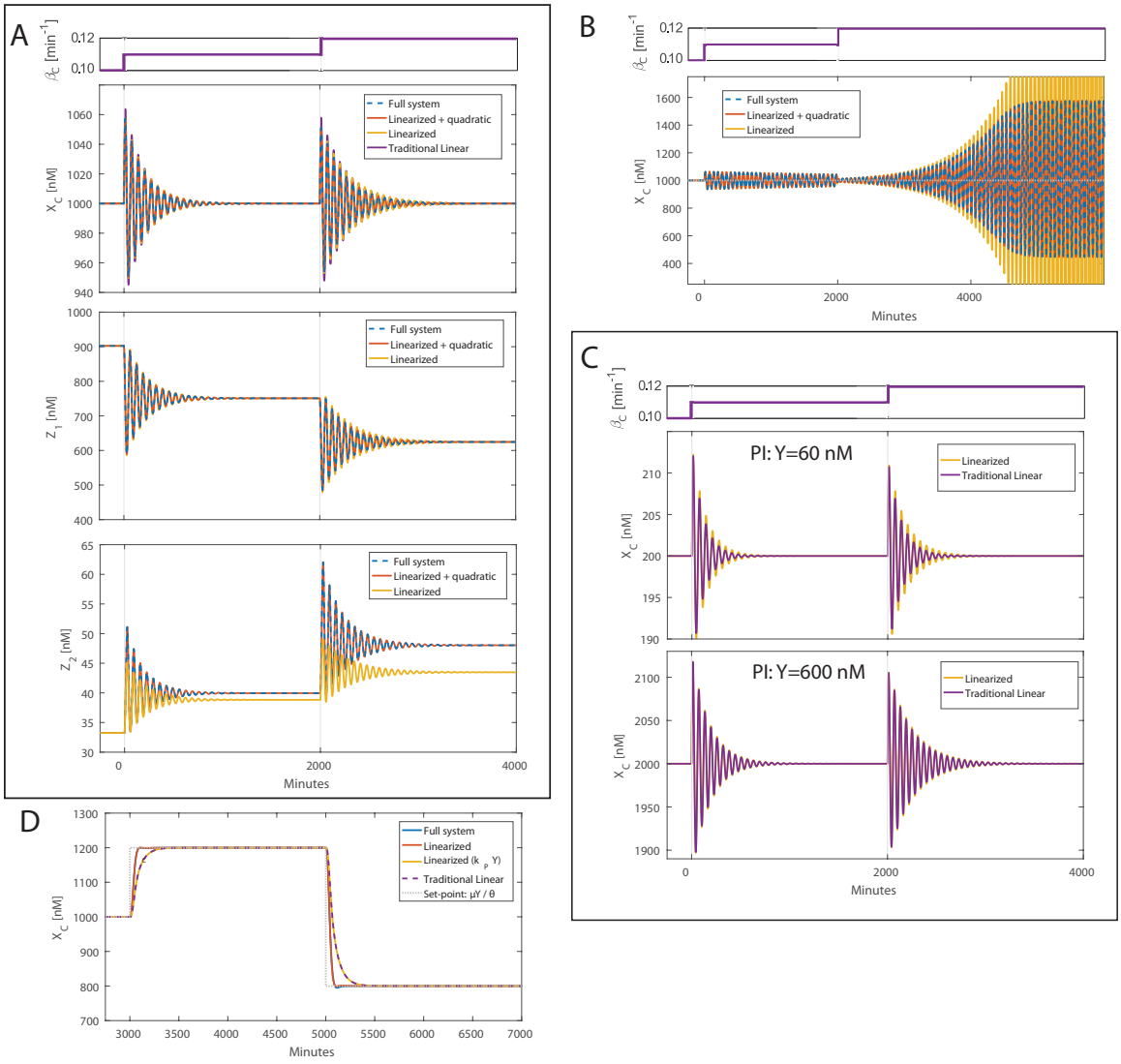

Figure S7: Related to Section "Linear perturbation analysis of nonlinear PID control design provides analytical support for the design", Section "PID benefits depend on the process to be controlled and PID gains need to be tuned", and STAR Methods "The control circuit equations linearized about a set-point". **Linearized biochemical PID control mimics the adaptation dynamics of the nonlinear controller for small to moderate step-changes in the parameter β_C and compares favorably to traditional PID controller under defined parameter regimes.** (A) The time dynamics of X_C, Z_1 and Z_2 are plotted for the full model (dashed blue, Eqs.(5-8,11-12)), the linearized model (yellow, Eq.(s22)), and the linearized model plus quadratic correction term, $\eta z_1(t) z_2(t)$ (red). See Table S2 for parameter values used in each simulation. The β_C perturbations are shown in the top panels. For X_C dynamics, the traditional PID case (purple) was simulated with just the process (Eq.(5)) and the X_1 equation with exact error terms (Eq.(s28)). (B) Linearized model (yellow) for the integral (I) only case, captures convergent oscillations (first change in β_C) and the onset of limit cycle (second change in β_C). Adding the quadratic term (red) agrees well with the full solution (dashed blue). (C) X_C dynamics for the linearized biochemical controller and traditional linear controller following step changes in β_C for $Y = 60\,\text{nM}$ (upper panel) and $Y = 600\,\text{nM}$ (lower panel). As Y increases, the two controllers converge as a result of the convergence of the k_I of the biochemical controller to that of the traditional controller. (D) X_C dynamics for the process with delay (no feedback) from Section "PID benefits depend on the process to be controlled and PID gains need to be tuned" (Figure 5A). In this case, the traditional PI controller output is not the same as that of the full nonlinear biochemical PI controller and its linearized model. However, changing the proportional terms from $3k_P Y$ to $k_P Y$ makes all the controllers indistinguishable, illustrating a difference between a traditional proportional controller and the biochemical one for this particular design.

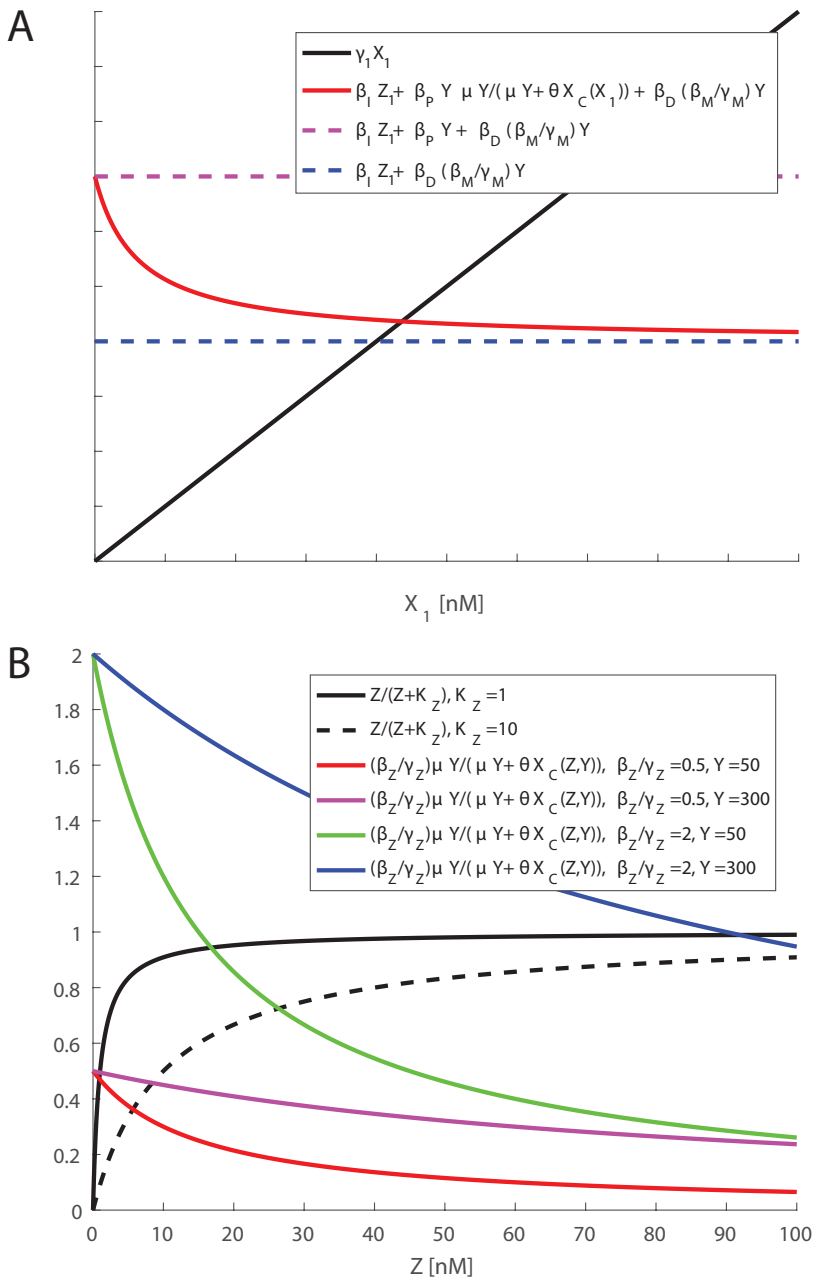

Figure S8: Related to Section "PID benefits depend on the process to be controlled and PID gains need to be tuned", Section "Constructing a PID controller with a different integral controller architecture", STAR Methods "Z_1 positively regulates X_C in the presence of P and D terms", and STAR Methods "Steady State analysis of integral controller from Eq. (25)". **Graphical solutions of steady-state Eq. (8) and steady-state Eq. (25).** (A) Uniqueness of solution for Eq. (8) between Z_1 and X_1 for the general PID case. As Z_1 increases, the crossing point of the two curves will increase in X_1. Thus, graphically proving that $dX_1/dZ_1 > 0$. (B) Graphical solutions of Eq. (25) for different values of β_Z/γ_Z, K_Z and Y. For $\beta_Z/\gamma_Z < 1$, solution will occur for $Z/(Z + K_Z) < \beta_Z/\gamma_Z$. Only for $\beta_Z/\gamma_Z > 1$ may the solution occur where $Z/(Z + K_Z) \approx 1$, the condition for approximate integral control. Results presented are for the I only case.